DALTON
FULL PAPER

Dinuclear, trinuclear and mixed-metal hexanuclear aggregates of vanadium: crystal structures and properties of $[NEt_4]_3[V_2Cl_9]$, $[PPh_4]_2[V_3OCl_4(O_2CC_6H_4SH)_5]$ and $[NEt_4]_4[V_2Li_4O_2Cl_4(O_2CC_6H_4S)_4]$ †

Gail B. Karet, Stephanie L. Castro, Kirsten Folting, John C. Bollinger, Robert A. Heintz and George Christou *

Department of Chemistry and Molecular Structure Center, Indiana University, Bloomington, IN 47405-4001, USA

The reaction between $[VCl_3(thf)_3]$ and Cl^- provided a high-yield route to $[NEt_4]_3[V_2Cl_9]$ **1**, which contains a $[V_2(\mu\text{-}Cl)_3Cl_6]^{3-}$ face-sharing bioctahedron. The reaction of $[VCl_3(thf)_3]$ with sodium 2-sulfanylbenzoate (mba^{2-}) in the presence of water and PPh_4Cl gave $[PPh_4]_2[V_3OCl_4(Hmba)_5]$ **2**, whose anion contains a triangular $[V_3(\mu_3\text{-}O)]^{7+}$ core. The reaction of $[NEt_4]_2[VOCl_4]$ with H_2mba and Li_2S gave $[NEt_4]_4[V_2Li_4O_2Cl_4(mba)_4]$ **3**, whose anion contains two [VO(mba)] fragments bridged by a $[Li_4Cl_4]$ unit. Compounds **1** and **2** are weakly antiferromagnetically coupled with $J = -13.4(4)$ and $-3.2(1.6)$ cm^{-1}, respectively ($\hat{H} = -2JS_iS_j$ convention).

We have been interested for some time in the synthesis and characterisation of vanadium complexes with a variety of nuclearities and ligand types and in the metal oxidation state range III–V, including mixed valency.[1–4] This interest has encompassed both the preparation of new structural types and a study of their spectroscopic and physical properties. Recently, a study of vanadium carboxylates was initiated and to date we have reported several species, including trinuclear $[V_3O(O_2CR)_6(py)_3]ClO_4$ (R = Me, Et, Ph, *etc.*; py = pyridine),[2] tetranuclear $[V_4O_2(O_2CEt)_7(bpy)_2]ClO_4$[3] (bpy = 2,2′-bipyridine) and $[NEt_4]_2[V_4O_8(NO_3)(O_2CC_4H_4S)_4]$,[4] and pentanuclear $[NR_4]_2[V_5O_9X(O_2CPh)_4]$ (X = Cl or Br),[4] together with their NMR, EPR, electrochemical and magnetic properties. In the present paper are described three species of differing nuclearity, two of which have resulted from attempts to incorporate a carboxylate derivative also containing a thiolate group, *i.e.* 2-sulfanylbenzoic acid (H_2mba), in the hope that the bifunctional ligand would yield new types of V_x products. Also described are a convenient preparation of the known $[NEt_4]_3[V_2Cl_9]$ in a form suitable for crystallography, and the magnetic characterisation of two V^{III}-containing complexes.

Experimental

General

All manipulations were performed under a purified argon atmosphere employing standard Schlenk and glove-box techniques. Acetonitrile, Et_2O and EtOH were distilled under argon from 4 Å molecular sieves, sodium–benzophenone solution, and ethyl Grignard, respectively. The compound $[VCl_3(thf)_3]$ (thf = tetrahydrofuran) was prepared from VCl_3 (Aldrich) as described in the literature.[5] $[NEt_4]_2[VOCl_4]$ from $VOSO_4\cdot nH_2O$, LiCl, and NEt_4Cl,[4] $Na_2[SC_6H_4CO_2]$ (Na_2mba) was prepared from sodium ethoxide and 2-sulfanylbenzoic acid (H_2mba, Aldrich) in EtOH. The 2-sulfanylbenzoic acid was used as received.

Preparations

$[NEt_4]_3[V_2Cl_9]$ 1. The compounds $[VCl_3(thf)_3]$ (0.74 g, 2.0 mmol) and $NBu^n{}_4Cl$ (0.83 g, 3.0 mmol) were dissolved in CH_2Cl_2 (20 cm^3) to give a purple solution. This was layered carefully with a solution of NEt_4Cl (0.50 g, 3.0 mmol) in CH_2Cl_2 (20 cm^3). Purple crystals of $\mathbf{1}\cdot 5CH_2Cl_2$ slowly formed as the two solutions mixed, and they were collected by filtration, washed with hexanes and dried *in vacuo*. The yield was 85%. Dried solid analysed as solvent-free (Found: C, 35.75; H, 7.53; Cl, 39.04; N, 5.07. $C_{24}H_{60}Cl_9N_3V_2$ requires C, 35.51; H, 7.45; Cl, 39.31; N, 5.17%).

$[PPh_4]_2[V_3OCl_4(Hmba)_5]$ 2. Acetonitrile (50 cm^3) was added to a Schlenk flask containing $[VCl_3(thf)_3]$ (1.21 g, 3.09 mmol) and Na_2mba (0.592 g, 2.98 mmol). The mixture was allowed to stir for 2 h, and then water (0.060 cm^3, 3.3 mmol) was added. The suspension was stirred overnight, during which time it turned grayish green. The resulting solution was filtered, and PPh_4Cl (0.975 g, 2.60 mmol) was added to the green filtrate. The resulting brown solution was filtered, and left undisturbed at room temperature. After 2–3 d large green blocks suitable for crystallographic study had crystallised. The crystals were filtered off, washed with EtOH (6 × 10 cm^3), and dried under vacuum. The yield was 0.61 g, (58%) based on mba^{2-} (Found: C, 56.7; H, 3.74; N, 0.15. $C_{83}H_{65}Cl_4O_{11}P_2S_5V_3\cdot 0.25CH_3CN$ requires C, 56.8; H, 3.75; N, 0.20%). Selected IR spectral data: 1603vs, 1578vs and 1549s (ν_{CO}).

$[NEt_4]_4[V_2Li_4O_2Cl_4(mba)_4]$ 3. The salt $[NEt_4]_2[VOCl_4]$ (1.40 g, 2.98 mmol), H_2mba (0.462 g, 3.00 mmol), and Li_2S (0.272 g, 6.00 mmol) were placed in a Schlenk flask, and MeCN (60 cm^3) was added by syringe. The mixture was stirred overnight, the resulting purple solution was filtered to remove gray solids, and the filtrate left undisturbed for 4 d. After this time the blue solution of the product was filtered to remove red solids, and the volume of the blue filtrate reduced to 35 cm^3. Slow diffusion of Et_2O (40 cm^3) into the filtrate produced blue crystals suitable for X-ray crystallographic studies along with some white powder of LiCl. The mass of isolated material was 0.78 g, (68% yield based on mba^{2-}) (Found: C, 47.09; H, 6.02; N, 3.64. $C_{60}H_{96}Cl_4N_4O_{10}S_4V_2\cdot 2LiCl$ requires C, 47.48; H, 6.38; N, 3.69%).

X-Ray crystallography

Data were collected at low temperature on a Picker four-circle

---

† *Non-SI unit employed*: $\mu_B \approx 9.27 \times 10^{-24}$ J T^{-1}.

diffractometer with graphite-monochromated Mo-Kα radiation (λ 0.710 69 Å); details of the diffractometry, low-temperature facilities, and computational procedures employed by the Indiana University MSC are available elsewhere.[6] Suitable crystals were located, affixed to glass fibers using silicone grease, and transferred to the goniostat where they were cooled for characterisation and data collection. Data were corrected for Lorentz-polarisation effects, and equivalent data averaged. The structures were solved by direct methods (MULTAN 78[7] and SHELXS 86[8]) and Fourier-difference techniques, and refined by full-matrix least-squares cycles.

For compound **1**·5CH$_2$Cl$_2$ a systematic search of a limited hemisphere of reciprocal space located a set of reflections with monoclinic symmetry and systematic absences corresponding to a C-centered cell. Subsequent successful solution and refinement of the structure confirmed the space group to be $C2$. Following data collection ($+h$, $+k$, $\pm l$; $6 \leqslant 2\theta \leqslant 45°$) and averaging of equivalent reflections ($R_{av} = 0.019$), the structure was solved without problem and all non-hydrogen atoms were readily located. All hydrogen atoms were readily located in a Fourier-difference map phased on the non-hydrogen atoms. In the final refinement (on F) cycles non-hydrogen atoms were refined anisotropically and all hydrogen atoms isotropically. The final Fourier-difference map was essentially featureless. Final $R(R')$ values are included in Table 1.

For complex **2**·2MeCN·C$_6$H$_{14}$ a systematic search of a limited hemisphere of reciprocal space located a set of intensities with monoclinic symmetry and systematic absences corresponding uniquely to the centrosymmetric space group $P2_1/a$. Following data collection ($+h$, $+k$, $\pm l$; $5 \leqslant 2\theta \leqslant 45°$) and averaging of equivalent reflections ($R_{av} = 0.067$), the structure was solved without problem and all non-hydrogen atoms readily located. In the final refinement cycles (on F^2) all non-hydrogen atoms were refined with anisotropic thermal parameters. All C–H hydrogen atoms were placed in calculated positions and refined with the use of a riding model. Some of the hydrogen atoms attached to the sulfur atoms were located in a Fourier-difference map phased on the non-hydrogen atoms, and these were included as fixed isotropic contributors in the final refinement cycles. The structure exhibits some disorder: three S atoms were disordered between the two *ortho* positions of the Ph rings to which they are attached (labelled A and B in the Supplementary Material) with occupancies of 40:60% for S(9A/B), 37:63% for S(29A/B), and 31:69% for S(39A/B). Some of the ring C atoms have somewhat elongated thermal parameters indicating some small measure of additional disorder that was not further modelled. In addition to the anions and cations, the asymmetric unit contained two well behaved, full-occupancy MeCN solvate molecules, and one disordered hexane molecule; for the latter, seven distinct C atoms were located and included, and their occupancies all refined to values in the range 46–73%. A final Fourier-difference map was essentially featureless, the largest peak being 0.82 e Å^{-3} near one of the sulfur atoms. Final $R(R')$ values are listed in Table 1.

For complex **3** a systematic search of a limited hemisphere of reciprocal space located a set of intensities which exhibited no Laue symmetry (other than $\bar{1}$). The choice of the triclinic space group $P\bar{1}$ was confirmed by the subsequent successful solution and refinement of the structure. Following data collection ($+h$, $\pm k$, $\pm l$; $6 \leqslant 2\theta \leqslant 45°$) and averaging of equivalent reflections ($R_{av} = 0.020$), the structure was solved without problem and all non-hydrogen atoms readily located and refined with anisotropic thermal parameters. Hydrogen atoms were introduced in fixed, calculated positions with isotropic thermal parameters equal to 1.0 plus the isotropic equivalent of the atom to which they are attached. The full unique data set was used for the refinement (on F); reflections having $F < 3.0\sigma(F)$ were given zero. A final Fourier-difference map was essentially featureless, the largest peak being 0.75 e Å^{-3} and the deepest hole being -0.48 e Å^{-3}. Final $R(R')$ values are listed in Table 1.

CCDC reference number 186/749.

Physical Measurements

Infrared spectra were recorded as Nujol mulls on CsI plates using a Nicolet 510P FTIR spectrophotometer. Variable-temperature magnetic measurements were made with a Quantum Design MPMS SQUID susceptometer at Michigan State University operating with a 10 kG (1 T) applied magnetic field.

Results and Discussion

Syntheses

The procedure to [NEt$_4$]$_3$[V$_2$Cl$_9$] **1** is a slightly modified version of that reported earlier, which involved direct addition of 3 equivalents of NEt$_4$Cl to a slurry of [VCl$_3$(thf)$_3$] in CH$_2$Cl$_2$ and gave sparingly soluble **1** as a microcrystalline solid.[9,10] In order to obtain large single crystals for crystallography, the [VCl$_3$(thf)$_3$] was first solubilized in CH$_2$Cl$_2$ with NBu$^n_4$Cl and then slow (diffusive) addition of NEt$_4$Cl gave slow formation of large crystals of **1**·5CH$_2$Cl$_2$. The overall reaction is summarised in equation (1). This route is superior in both convenience and yield to those employed for [NH$_2$Et$_2$]$_3$[V$_2$Cl$_9$],[11] [N(SCl)$_2$]$_3$[V$_2$Cl$_9$][12] and [PPh$_4$]$_3$[V$_2$Cl$_9$].[13] The compound Cs$_3$V$_2$Cl$_9$ is available from a high-temperature solid-state route.[14]

$$2\,[\mathrm{VCl_3(thf)_3}] + 3\,\mathrm{NEt_4Cl} \longrightarrow [\mathrm{NEt_4}]_3[\mathrm{V_2Cl_9}] + 6\,\mathrm{thf} \quad (1)$$

The reaction of [VCl$_3$(thf)$_3$] with Na$_2$mba was designed as a potential route to vanadium(III) complexes with mixed O/S ligation, but instead gave the unusual complex [PPh$_4$]$_2$[V$_3$OCl$_4$(Hmba)$_5$] **2**. The thiolate functions have been protonated (see below) and this probably facilitates formation of an O^{2-}-containing product from H$_2$O molecules; we have shown elsewhere that the presence of thiolate groups to act as Brønsted bases facilitates the incorporation of O^{2-} ions from H$_2$O into a V$_x$ product.[1c] The yield was increased to 58% (based on mba^{2-}) by deliberate addition of water, but attempts to increase the yield further by using a rational V:mba^{2-} ratio of 3:5 were unsuccessful, giving a mixture of products; the sub-stoichiometric quantities appear essential for clean formation of **2**.

The reaction of [NEt$_4$]$_2$[VOCl$_4$] with H$_2$mba and Li$_2$S was another attempt to introduce V–S linkages, but the S^{2-} ion again appeared to act as a Brønsted base, and the product was [NEt$_4$]$_4$[V$_2$Li$_4$O$_2$Cl$_4$(mba)$_4$] **3**. As for **2**, attempts to optimise yield by employing a rational V:mba^{2-} ratio of 2:4 gave a mixture of V-containing products, as did reactions in which the Li$_2$S was omitted. In complex **3** the mba group did now chelate, producing a mixed O/S-ligated vanadium complex.

Crystal structures

The ORTEP[15] representations of the anions of complexes **1**, **2** and **3** are shown in Figs. 1–3, respectively. Selected interatomic distances and angles are listed in Tables 2–4.

Compound **1**·5CH$_2$Cl$_2$ crystallises in monoclinic space group $C2$. The anion is a face-sharing bioctahedron lying on a crystallographic C_2 axis passing through Cl(6) and the midpoint of the V(1)–V(1′) vector; the virtual symmetry is D_{3h}. The V$^{III}\cdots$V^{III} distance [3.279(2) Å] precludes a metal–metal bond, and the bridging V–Cl bonds [average 2.472(2) Å] are longer than terminal ones [average 2.321(2) Å], as expected. The corresponding distances in [PPh$_4$]$_3$[V$_2$Cl$_9$] are 3.275(3), 2.451(3) and 2.341(3) Å,[13] indicating little dependence on cation identity. The corresponding titanium(III) complex [NEt$_4$]$_3$[Ti$_2$Cl$_9$]·5CH$_2$Cl$_2$ was recently reported[16] and is isomorphous with **1**·5CH$_2$Cl$_2$; the Ti$\cdots$Ti separation [3.216(5) Å] is slightly shorter than that in **1**.

Table 1 Crystallographic data for complexes **1**·5CH_2Cl_2, **2**·2MeCN·C_6H_{14} and **3**

	1	**2**	**3**
Formula[a]	$C_{29}H_{70}Cl_9N_3V_2$	$C_{87}H_{71}Cl_4N_2O_{11}P_2S_5V_3$[a]	$C_{60}H_{96}Cl_4Li_4N_4O_{10}S_4V_2$
M	1236.4	1837.4	1433.1
Crystal symmetry	Monoclinic	Monoclinic	Triclinic
Space group	*C*2	$P2_1/a$	$P\bar{1}$
a/Å	18.032(3)	23.565(2)	12.238(4)
b/Å	13.875(2)	13.727(1)	14.518(4)
c/Å	11.718(2)	26.347(2)	10.310(3)
α/°			100.21(2)
β/°	113.99(1)	95.05(1)	93.14(2)
γ/°			85.66(2)
U/Å^3	2678.6	8489.6	1796.0
Z	2	4	1
T/°C	−171	−171	−170
D_c/g cm^{-3}	1.533	1.438	1.325
μ/cm^{-1}	13.215	6.49	5.65
Unique data	1845	11 155	4694
Observed data	1747[b]	7000[c]	4073[d]
R(*R*′)	0.0230 (0.1156)[e,f]	0.0529 (0.1156)[e,g]	0.0405 (0.0447)[e,f]

[a] Including 2MeCN molecules only. [b] $F > 2.33\sigma(F)$. [c] $F > 4\sigma(F)$. [d] $F > 3\sigma(F)$. [e] $R = \Sigma\|F_o| - |F_c\|/\Sigma|F_o|$. [f] $R'(F) = [\Sigma w(|F_o| - |F_c|)^2/\Sigma w|F_o|^2]^{\frac{1}{2}}$ where $w = 1/\sigma^2(|F_o|)$. [g] $R'(F^2) = [\Sigma w(F_o^2 - F_c^2)^2/\Sigma w(F_o^2)^2]^{\frac{1}{2}}$.

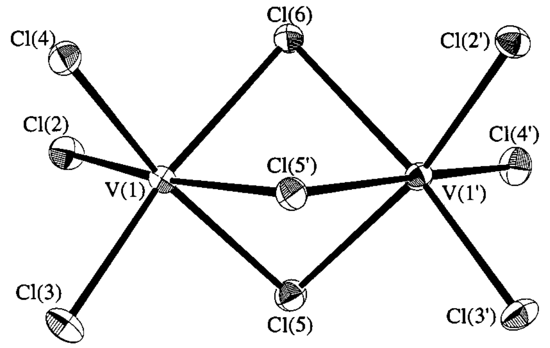

Fig. 1 An ORTEP representation of the anion of complex **1**. Thermal ellipsoids are at the 50% probability level. Primed and unprimed atoms are related by a two-fold rotation axis through Cl(6)

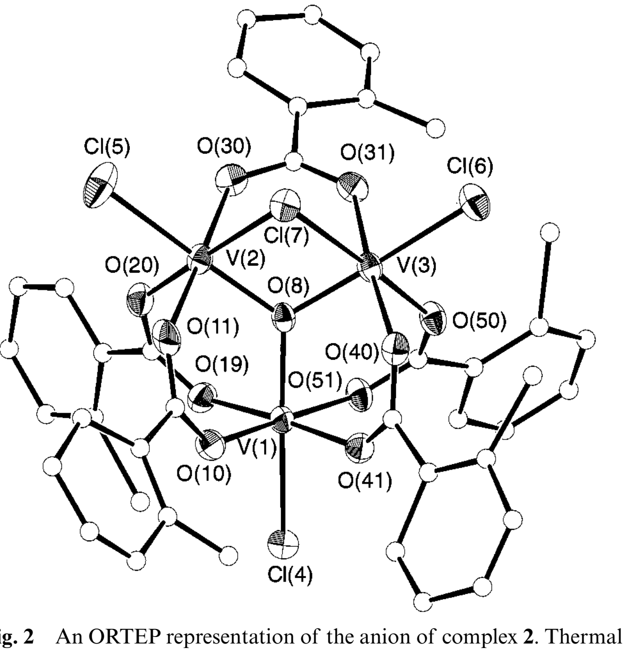

Fig. 2 An ORTEP representation of the anion of complex **2**. Thermal ellipsoids are at the 50% probability level, except for the C and S atoms of the Hmba$^-$ groups, which are shown as isotropic spheres of arbitrary size

Compound **2** crystallises in monoclinic space group $P2_1/a$. The anion has no crystallographically imposed symmetry and consists of an oxide-centred triangular $[V^{III}_3O]^{7+}$ unit. The V_2 edges are bridged by a total of six groups, five of which are Hmba$^-$ carboxylates in the familiar *syn*,*syn*,μ mode and the sixth a μ-Cl$^-$ ion. Six-co-ordination at each vanadium(III) centre is completed by a terminal Cl$^-$ ion. If the S atoms on the Hmba$^-$ groups are ignored, the anion has virtual C_s symmetry with the mirror plane passing through atoms Cl(4), V(1), O(8), Cl(7) and three C atoms of one Hmba$^-$ group. The asymmetry introduced by the single μ-Cl$^-$ ion causes the V_3 triangle to be virtually isosceles rather than equilateral with the V(2)···V(3) separation [3.123(2) Å] being significantly shorter than V(1)···V(2) [3.360(2) Å] and V(1)···V(3) [3.391(2) Å]. The bridging V–Cl(7) lengths (average 2.455 Å) and V(2)–Cl(7)–V(3) angle [78.99(5)°] in **2** are statistically the same and slightly more acute, respectively, than corresponding parameters for the bridging Cl$^-$ ions **1** (averages 2.472 Å and 82.84°). Similarly, the terminal V–Cl lengths of **2** (average 2.359 Å) are slightly longer than those in **1** (average 2.321 Å). The more acute V–Cl–V angle and lengthened terminal V–Cl bonds in **2** *vs.* **1** may both reasonably be attributed to the short V–O bonds (≈1.90 Å) and an increased *trans* influence resulting from the μ_3-O^{2-} ion.

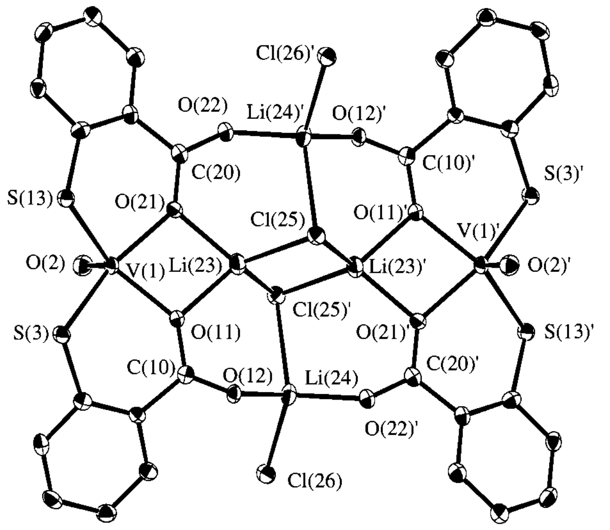

Fig. 3 An ORTEP representation of the anion of complex **3**. Thermal ellipsoids are at the 50% probability level. Primed and unprimed atoms are related by an inversion centre

The structure of the anion of complex **2** is distinctly different from that of all previously characterised triangular V^{III}_3 (or

Table 2 Selected interatomic distances (Å) and angles (°) for $[NEt_4]_3[V_2Cl_9]\cdot5CH_2Cl_2$ (**1**·$5CH_2Cl_2$)

V(1)···V(1′)	3.279(2)	V(1)–Cl(5)	2.449(2)
V(1)–Cl(2)	2.330(2)	V(1)–Cl(5′)	2.471(2)
V(1)–Cl(3)	2.300(2)	V(1)–Cl(6)	2.497(2)
V(1)–Cl(4)	2.333(2)		

Cl(2)–V(1)–Cl(3)	94.57(5)	Cl(4)–V(1)–Cl(5′)	89.82(5)
Cl(2)–V(1)–Cl(4)	95.09(5)	Cl(4)–V(1)–Cl(5)	169.79(5)
Cl(2)–V(1)–Cl(5)	169.17(6)	Cl(4)–V(1)–Cl(6)	93.22(5)
Cl(2)–V(1)–Cl(5′)	93.23(5)	Cl(5)–V(1)–Cl(5)	81.00(5)
Cl(2)–V(1)–Cl(6)	89.58(5)	Cl(5′)–V(1)–Cl(6)	80.49(4)
Cl(3)–V(1)–Cl(4)	93.31(5)	Cl(5)–V(1)–Cl(6)	80.92(4)
Cl(3)–V(1)–Cl(5′)	94.78(5)	V(1)–Cl(5)–V(1)	83.60(5)
Cl(3)–V(1)–Cl(5)	91.91(5)	V(1)–Cl(6)–V(1)	82.07(7)
Cl(3)–V(1)–Cl(6)	171.92(6)		

Table 3 Selected interatomic distances (Å) and angles (°) for $[PPh_4]_2[V_3OCl_4(Hmba)_5]$ **2**

V(1)···V(2)	3.360(2)	V(2)–O(11)	2.023(3)
V(1)···V(3)	3.391(2)	V(2)–O(20)	2.028(3)
V(2)···V(3)	3.123(2)	V(2)–Cl(5)	2.370(2)
V(1)–O(8)	1.911(3)	V(2)–Cl(7)	2.439(2)
V(1)–O(19)	1.998(4)	V(3)–O(8)	1.905(3)
V(1)–O(51)	2.012(3)	V(3)–O(40)	1.988(4)
V(1)–O(41)	2.017(4)	V(3)–O(31)	1.996(4)
V(1)–O(10)	2.026(3)	V(3)–O(50)	2.018(4)
V(1)–Cl(4)	2.354(2)	V(3)–Cl(6)	2.353(2)
V(2)–O(8)	1.904(3)	V(3)–Cl(7)	2.472(2)
V(2)–O(30)	2.016(3)		

O(8)–V(1)–O(19)	91.94(14)	O(41)–V(1)–O(10)	176.1(2)
O(8)–V(1)–O(51)	91.50(14)	O(8)–V(1)–Cl(4)	178.11(11)
O(19)–V(1)–O(51)	176.42(2)	O(19)–V(1)–Cl(4)	87.80(11)
O(8)–V(1)–O(41)	89.94(14)	O(51)–V(1)–Cl(4)	88.79(11)
O(19)–V(1)–O(41)	86.19(14)	O(41)–V(1)–Cl(4)	91.91(11)
O(51)–V(1)–O(41)	92.8(2)	O(10)–V(1)–Cl(4)	88.53(11)
O(8)–V(1)–O(10)	89.60(13)	O(8)–V(2)–O(30)	89.91(14)
O(19)–V(1)–O(10)	89.93(14)	O(8)–V(2)–O(11)	93.24(14)
O(51)–V(1)–O(10)	91.10(14)	O(30)–V(2)–O(11)	86.65(14)
O(8)–V(2)–O(20)	92.61(14)	O(40)–V(3)–O(50)	93.7(2)
O(30)–V(2)–O(20)	175.40(14)	O(31)–V(3)–O(50)	85.51(14)
O(11)–V(2)–O(20)	89.36(14)	O(8)–V(3)–Cl(6)	175.68(11)
O(8)–V(2)–Cl(5)	177.03(11)	O(40)–V(3)–Cl(6)	88.49(12)
O(30)–V(2)–Cl(5)	90.71(11)	O(31)–V(3)–Cl(6)	90.65(11)
O(11)–V(2)–Cl(5)	89.69(11)	O(50)–V(3)–Cl(6)	90.20(11)
O(20)–V(2)–Cl(5)	86.97(11)	O(8)–V(3)–Cl(7)	81.55(10)
O(8)–V(2)–Cl(7)	82.44(10)	O(40)–V(3)–Cl(7)	92.23(11)
O(30)–V(2)–Cl(7)	90.34(11)	O(31)–V(3)–Cl(7)	88.64(11)
O(11)–V(2)–Cl(7)	174.75(11)	O(50)–V(3)–Cl(7)	172.59(11)
O(20)–V(2)–Cl(7)	93.81(10)	Cl(6)–V(3)–Cl(7)	94.42(6)
Cl(5)–V(2)–Cl(7)	94.66(5)	V(2)–Cl(7)–V(3)	78.99(5)
O(8)–V(3)–O(40)	90.13(14)	V(2)–O(8)–V(3)	110.2(2)
O(8)–V(3)–O(31)	90.79(14)	V(2)–O(8)–V(1)	123.4(2)
O(40)–V(3)–O(31)	178.8(2)	V(3)–O(8)–V(1)	125.4(2)
O(8)–V(3)–O(50)	93.97(14)		

Table 4 Selected interatomic distances (Å) and angles (°) for $[NEt_4]_4[V_2Li_4O_2Cl_4(mba)_4]$ **3**

V(1)···Li(23)	3.036(4)	Cl(26)–Li(24)	2.317(6)
Li(23)···Li(23′)	2.916(7)	S(3)–C(4)	1.765(4)
Li(23)···Li(24′)	3.358(7)	S(13)–C(14)	1.767(4)
V(1)–S(3)	2.350(1)	O(11)–C(10)	1.306(4)
V(1)–S(13)	2.336(1)	O(11)–Li(23)	1.972(6)
V(1)–O(2)	1.594(3)	O(12)–C(10)	1.229(4)
V(1)–O(11)	1.989(2)	O(12)–Li(24)	1.963(6)
V(1)–O(21)	1.996(2)	O(21)–C(20)	1.297(4)
Cl(25)–Li(23)	2.327(6)	O(21)–Li(23)	1.970(6)
Cl(25)–Li(23′)	2.341(6)	O(22)–C(20)	1.239(4)
Cl(25)–Li(24′)	2.482(6)	O(22)–Li(24)	1.919(6)

S(3)–V(1)–S(13)	84.56(4)	O(11)–V(1)–O(21)	78.81(10)
S(3)–V(1)–O(2)	105.68(10)	Li(23)–Cl(25)–Li(23′)	77.33(23)
S(3)–V(1)–O(11)	87.76(8)	Li(23)–Cl(25)–Li(24′)	88.53(21)
S(3)–V(1)–O(21)	149.43(8)	Li(23)–Cl(25′)–Li(24)	90.76(21)
S(13)–V(1)–O(2)	110.05(10)	V(1)–O(11)–Li(23)	100.09(21)
S(13)–V(1)–O(11)	138.95(8)	C(10)–O(11)–Li(23)	120.90(27)
S(13)–V(1)–O(21)	87.78(8)	C(10)–O(12)–Li(24)	131.63(28)
O(2)–V(1)–O(11)	110.86(12)	V(1)–O(21)–Li(23)	99.94(20)
O(2)–V(1)–O(21)	104.75(12)	C(20)–O(21)–Li(23)	123.22(28)
Cl(25)–Li(23)–Cl(25′)	102.67(23)	Cl(25′)–Li(24)–Cl(26)	119.00(25)
Cl(25′)–Li(23)–O(11)	106.23(27)	Cl(25′)–Li(24)–O(12)	100.80(25)
Cl(25)–Li(23)–O(11)	131.4(3)	Cl(25′)–Li(24)–O(22′)	104.49(26)
Cl(25′)–Li(23)–O(21)	126.9(3)	Cl(26)–Li(24)–O(12)	105.86(26)
Cl(25)–Li(23)–O(21)	111.8(3)	Cl(26)–Li(24)–O(22′)	109.09(27)
O(11)–Li(23)–O(21)	79.85(24)	O(12)–Li(24)–O(22′)	118.1(3)

$V^{II}V^{III}{}_2$) carboxylate complexes. The $[V_3O(O_2CR)_6L_3]^{0,+}$ (R/L = CF_3/thf,[17] CH_3/py,[17] CH_3/thf,[17] CH_2Cl/H_2O,[17,18] Et/4-methylpyridine[2]) species possess virtual D_{3h} symmetry with a $[V_3(\mu_3\text{-}O)]^{7+}$ core and two RCO_2^- groups bridging each V_2 edge; only in **2**, charged groups (Cl^-) are found at the terminal positions. More related to **2** is the non-carboxylate $V^{III}{}_3$ complex $[V_3OCl_7(PhHNNH_2)_4(thf)]$[19] where a triangular $[V_3(\mu_3\text{-}O)]^{7+}$ core has bridging $PhHNNH_2$ on two edges and a μ-Cl on the third, with two terminal Cl^- ions on each V^{III}. The triangular cobalt(III) complex $[Co_3O(OH)(O_2CMe)_5(py)_3]^+$ has, like **2**, five bridging RCO_2^- and one monoatomically bridging (OH^-) group.[20]

Compound **3** crystallises in triclinic space group $P\bar{1}$ with the anion lying on an inversion centre at the intersection of the Li(23)–Li(23′) and Cl(25)–Cl(25′) vectors. The anion consists of two $[VO(mba)_2]^{2-}$ units held together by a $[Li_4Cl_4]$ central unit, the latter comprising two edge-sharing, Cl^--capped Li_3 triangles. The resulting assembly has a planar, raft-like structure. The V(1)–O(2) distance [1.594(3) Å] is as expected for a $[VO]^{2+}$ triply bonded unit, and the tetraanionic nature of the ion is consistent with the S atoms not being protonated. The V(1)···V(1′) distance is 8.962(3) Å.

Magnetic susceptibility studies

Variable-temperature, solid-state, magnetic susceptibility (χ_m) studies have been performed on powdered samples of compounds **1** and **2** in the temperature range 5.00–360 K. Such studies were not performed on **3** given the large separation between the vanadium(IV) ions.

For compound **1**, the effective magnetic moment (μ_{eff}) per V_2 anion slowly decreases from 3.75 μ_B at 360 K to 1.67 μ_B at 5.00 K. These correspond to $\chi_m T$ values of 1.76 and 0.35 $cm^3\ K\ mol^{-1}$, respectively. The spin-only ($g = 2$) μ_{eff} and $\chi_m T$ values for a $V^{III}{}_2$ unit with non-interacting vanadium(III) ions are 4.00 μ_B and 2.00 $cm^3\ K\ mol^{-1}$, respectively, indicating the presence of an antiferromagnetic exchange interaction in **1**. Attempts to fit the data using the theoretical χ_m *vs.* T expression derived employing the Heisenberg spin Hamiltonian $\hat{H} = -2J\hat{S}_1\cdot\hat{S}_2$ encountered the same problems as previous studies of the $[NEt_4]_3[V_2Cl_9]$ compound, namely the inability to get a good fit of the data over the entire temperature range.[21] This has long been recognised as due to the $^3T_{1g}$ ground state of V^{III} in O_h symmetry and the resulting presence of unquenched orbital angular momentum,[21,22] making inaccurate the application of the Heisenberg spin Hamiltonian which assumes only spin angular momentum is present; although the local symmetry of each vanadium(III) ion in **1** is formally C_{3v}, the extent of distortion away from O_h symmetry is nevertheless relatively minor. However, using only the 80–360 K data, where the changing populations of the $S = 0$, 1, 2 states of the molecule should dominate the χ_m *vs.* T behaviour, a good fit was obtained with $J = -13.4(4)\ cm^{-1}$ and $g = 1.744(3)$, and employing a fixed temperature-independent paramagnetism (t.i.p.) term of $800 \times 10^{-6}\ cm^3\ K\ mol^{-1}$; a paramagnetic impurity contribution should be insignificant at these temperatures and it was omitted from the fit. These values are similar to those ($J \approx -20\ cm^{-1}$,

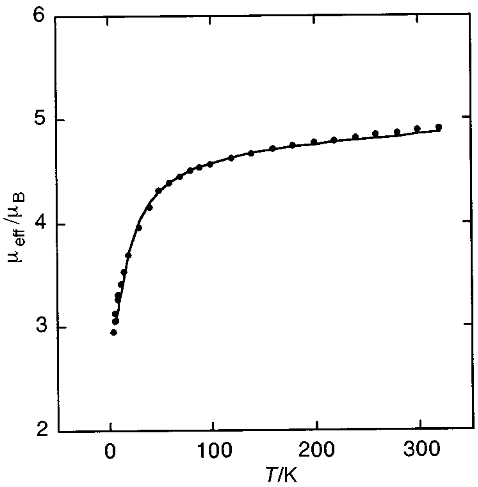

Fig. 4 Plot of effective magnetic moment (μ_{eff}) per V_3 *vs.* temperature for $[PPh_4]_2[V_3OCl_4(Hmba)_5]$ **2**. The solid line is a fit of the data by an equilateral (one-J) model; see the text for the fitting parameters

$g = 1.79$) previously estimated for **1** by Casey and Clark.[21] Thus, both studies on **1** are consistent with a weakly antiferromagnetic interaction. Note, however, that the exchange interactions in $Cs_3V_2Cl_9$ and $Rb_3V_2Br_9$ have been concluded to be ferromagnetic from inelastic neutron scattering and magnetic circular dichroism studies.[23] We have also previously reported the crystal structure and magnetic properties of the related complex $[NEt_4][V_2Cl_7(thf)_2]$[24] where two terminal Cl^- ions have been replaced by thf groups; this lowering of symmetry led to better fits of the data using the Heisenberg spin Hamiltonian, giving $J = -48(1)$ cm^{-1} and $g = 1.90$. The stronger interaction in the $[V_2Cl_7(thf)_2]^-$ ion compared with that in **1** may be due, at least in part, to the shorter V···V separation in the former [3.176(2) Å] than in the latter [3.279(2) Å] giving greater direct overlap of the magnetic orbitals.

For compound **2** the μ_{eff} value per V_3 unit steadily decreases from 4.91 μ_B at 320 K to 2.95 μ_B at 5.00 K (Fig. 4), corresponding to $\chi_m T$ values of 3.01 and 1.09 cm^3 K mol^{-1}, respectively. The spin-only μ_{eff} for a triangle of non-interacting vanadium(III) ions is 4.90 μ_B, suggesting the presence of weak antiferromagnetic exchange interactions in **2**.

On the basis of the virtual C_s symmetry of the anion of complex **2**, the data were fitted by the theoretical χ_m *vs.* T expression derived elsewhere for an isosceles triangle of three $S = 1$ vanadium(III) ions.[2] The spin Hamiltonian and resultant energy expression for such a system are given in equations (2)

$$\hat{H} = -J(\hat{S}_T{}^2 - \hat{S}_A{}^2 - \hat{S}_1{}^2) - J'(\hat{S}_A{}^2 - \hat{S}_2{}^2 - \hat{S}_3{}^2) \quad (2)$$

and (3), respectively, where $\hat{S}_1$, $\hat{S}_2$ and $\hat{S}_3$ are the spin operators

$$E(S_T, S_A) = -J[S_T(S_T + 1) - S_A(S_A + 1)] - J'[S_A(S_A + 1)] \quad (3)$$

for V(1), V(2) and V(3), respectively, $\hat{S}_A = \hat{S}_2 + \hat{S}_3$ and $\hat{S}_T = \hat{S}_A + \hat{S}_1$; S_T is the total spin of the V_3 unit. Fitting of the data using this χ_m *vs.* T expression gave a good fit with $J = J_{12} = J_{13} = 0.3$ cm^{-1}, $J' = J_{23} = -7.3$ cm^{-1}, and $g = 1.97$, and t.i.p. held constant at 600×10^{-6} cm^3 K mol^{-1}. However, the uncertainty in the J and J' values was clearly high when a relative error surface for the fitting was examined as a function of J and J'. This showed the minimum to lie in an essentially flat trough or valley within which essentially equally good fits could be obtained for $J = +5$ to -3 cm^{-1} and $J' = -12$ to -2 cm^{-1}, with the two values correlated. As a result the fitting parameters often varied from run to run, and were very sensitive to a number of factors, including small changes to g and the low-temperature cut-off for data used (5, 7 or 9 K, for example). We conclude that although there probably is a real difference between J and J', neither their values nor their difference can be determined accurately or precisely from our fitting procedure, given the estimated uncertainties in J and J' of ± 3 cm^{-1} at least. Thus, even the use of an isosceles triangle model may be considered as unjustified, and for comparison purposes, the data (5.00–320 K) were also fitted by an equilateral triangle model ($J = J'$) giving a good fit with $J = -3.2$ (1.6) cm^{-1}, $g = 1.92(3)$ and t.i.p. held at 600×10^{-6} cm^3 K mol^{-1}. This fit is shown as the solid line in Fig. 4. We believe that the only safe conclusion to be made is that the exchange interactions in **2** are all very weakly antiferromagnetic, giving an $S_T = 0$ ground state. Note that this is similar to the ground state found for $[V_3O(O_2CMe)_6(py)_3]ClO_4$ where stronger exchange interactions [$J = -18.0(7)$, $J' = -10.4(4)$ cm^{-1}] and more precise fits of the data were obtained.[2]

Conclusion

The present work has shown that treatment of $[VCl_3(thf)_3]$ with Cl^- followed by a slow-cation exchange procedure provides a convenient route to large yields of pure, highly crystalline $[NEt_4]_3[V_2Cl_9]$ that also allow structural characterisation. The same procedure was recently also found successful for $[NEt_4]_3$-$[Ti_2Cl_9]$. The use of the mixed-function carboxylate/thiolate mba^{2-} allows access to a new type of triangular $V^{III}{}_3$ complex, the thiolate groups acting only as Brønsted bases. At the vanadium(IV) level, mba^{2-} does act as an O/S chelating ligand yielding a typical square-pyramidal $[VO(mba)_2]^{2-}$ unit which, however, forms a raft-like mixed-metal aggregate with LiCl. The present work supports our continuing belief that vanadium carboxylate cluster chemistry continues to represent a rich source of new structural types.

Acknowledgements

This work was supported by the U.S. Department of Energy under grant ER 13702.

References

1 (*a*) N. S. Dean, S. L. Bartley, W. E. Streib, E. B. Lobkovsky and G. Christou, *Inorg. Chem.*, 1995, **34**, 1608; (*b*) J. G. Reynolds, S. C. Sendlinger, A. M. Murray, J. C. Huffman and G. Christou, *Inorg. Chem.*, 1995, **34**, 5745; (*c*) J. R. Rambo, S. L. Castro, K. Folting, S. L. Bartley, R. A. Heintz and G. Christou, *Inorg. Chem.*, 1996, **35**, 6844.

2 S. L. Castro, W. E. Streib, J.-S. Sun and G. Christou, *Inorg. Chem.*, 1996, **35**, 4462.

3 S. L. Castro, Z. Sun, J. C. Bollinger, D. N. Hendrickson and G. Christou, *J. Chem. Soc., Chem. Commun.*, 1995, 2517.

4 G. B. Karet, Z. Sun, D. D. Heinrich, J. K. McCusker, K. Folting, W. E. Streib, J. C. Huffman, D. N. Hendrickson and G. Christou, *Inorg. Chem.*, 1996, **35**, 6450.

5 L. E. Manzer, *Inorg. Synth.*, 1982, **21**, 138.

6 M. H. Chisholm, K. Folting, J. C. Huffman and C. C. Kirkpatrick, *Inorg. Chem.*, 1984, **23**, 1021.

7 P. Nair, S. J. Fiske, S. E. Hull, L. Lessinger, G. Germain, J.-P. Declercq and M. M. Wolfson, MULTAN 78, Universities of York and Louvain, 1978.

8 G. M. Sheldrick, SHELXS 86, University of Göttingen, 1986.

9 R. J. H. Clark, R. S. Nyholm and D. E. Scaife, *J. Chem. Soc. A*, 1966, 1296.

10 A. T. Casey, R. J. H. Clark, W. Rhine, T. E. Boyd and G. Stucky, *Inorg. Synth.*, 1971, **13**, 168.

11 P. C. Crouch, G. W. A. Fowles and R. A. Walton, *J. Chem. Soc. A*, 1969, 972.

12 G. Beber, J. Hanich and K. Dehnicke, *Z. Naturforsch., Teil B*, 1985, **40**, 9.

13 K. Ruhlandt-Senge, A. D. Bacher, G. Koellner, B. Siewert and U. Muller, *Z. Naturforsch., Teil B*, 1992, **47**, 814.

14 A. Stebler, B. Leuenberger and H. U. Güdel, *Inorg. Synth.*, 1986, **26**, 377.

15 C. K. Johnson, ORTEP II, Report ORNL 5138, Oak Ridge National Laboratory, Oak Ridge, TN, 1976.
16 S. L. Castro, W. E. Streib, J. C. Huffman and G. Christou, *Chem. Commun.*, 1996, 2177.
17 F. A. Cotton, M. W. Extine, L. R. Falvello, D. B. Lewis, G. E. Lewis, C. A. Murillo, W. Schwotzer, M. Tomas and J. M. Troup, *Inorg. Chem.*, 1986, **25**, 3505.
18 T. Glowiak, M. Kubiak and B. Jezowska-Trzebiatowska, *Bull. Acad. Pol. Sci.*, *Ser. Sci. Chim.*, 1977, **25**, 359.
19 H. H. Murray, S. G. Novick, W. H. Armstrong and C. S. Day, *J. Cluster Sci.*, 1993, **4**, 439.
20 C. E. Summer, jun. and G. R. Steinmetz, *J. Am. Chem. Soc.*, 1985, **107**, 6124.
21 A. T. Casey and R. J. H. Clark, *Inorg. Chem.*, 1968, **7**, 1598.
22 B. Leuenberger and H. U. Güdel, *Mol. Phys.*, 1984, **51**, 1; *Inorg. Chem.*, 1986, **25**, 181.
23 B. Leuenberger, B. Briat, J. C. Canit, A. Furrer, P. Fischer and H. U. Güdel, *Inorg. Chem.*, 1986, **25**, 2930.
24 J. R. Rambo, S. L. Bartley, W. E. Streib and G. Christou, *J. Chem. Soc.*, *Dalton Trans.*, 1984, 1813.

Received 6th *August* 1997; *Paper* 7/05752K